Mapping of Magnetic field Inhomogeneity and Removal of its Artifact from MR Images

Abbas N. Moghaddam,[1,2] Hamid Soltanian-Zadeh[1,3]
[1]Electrical and Computer Engineering Department, University of Tehran, Tehran 14395-515, Iran
[2]CVIA lab, Washington University Medical Center, St. Louis, MO 63110,USA
[3]Radiology Department, Henry Ford Health System, Detroit, MI 48202, USA

ABSTRACT

Inhomogeneity of static magnetic field, induced by object susceptibility, is unavoidable in magnetic resonance imaging (MRI). This inhomogeneity generates distortions in both image geometry and its intensity. Based on node magnetic voltage values, a fast Finite Difference Method (FDM) is developed for susceptibility-induced mapping of magnetic field inhomogeneity and applied to simulated MRI data. Its accuracy and speed of convergence are evaluated by comparing the method to Finite Elements Method (FEM), which had been validated experimentally. Effects of inhomogeneity on Spin Echo (SE) MRI are simulated using the proposed field calculation method. Also, a pixel based (direct) method as well as a grid based (indirect) method for removing the effects are developed. The fast execution of the algorithm stems from the multi-resolution nature of the proposed method. The main advantage of the proposed method is that it does not need any data except for the image itself. Efficiency of both correction methods in distortion removal is investigated.

Keywords: Magnetic field inhomogeneity, Magnetic Resonance Imaging – MRI, geometrical distortion, Intensity distortion.

1. INTRODUCTION

Magnetic resonance, which has a great performance in soft tissue imaging, is very sensitive to magnetic field inhomogeneities. The large value of gyromagnetic coefficient causes a significant frequency shift even for few parts per million (ppm) field inhomogeneity, which in turn causes distortions in both geometry and intensity of the MR images. Field inhomogeneity may be produced by scanner as well as the object being imaged and therefore is not avoidable.
In recent years, many researchers have addressed this problem in their studies and tried to analyze and reduce its artifacts in MR images [1, 2, 3, 4, 5, 6]. These studies begin from pure theoretical investigations [2] and continue in numerical methods and different kinds of modeling and simulation [3, 7] and even improving hardware of MR system [8].

There are some general approaches for reducing field inhomogeneity induced artifacts like increasing the strength of gradient magnetic field, decreasing Echo Time (TE), improving the resolution of images and using phase encoding. On the other hand, many post-processing methods have been developed for removal of this artifact in which maps of magnetic field inhomogeneity are used.

In this research, we propose a method that extracts the mentioned map from distorted MR images, and then reduces the related artifacts. This method is developed for susceptibility induced inhomogeneity and Spin Echo imaging, but can be combined with other methods [9].

2. THEORY

2.1 Susceptibility induced magnetic field inhomogeneity

Homogeneity of the magnetic field is very important in acquiring MR Images. Manufacturers try to make the magnetic field as homogeneous as possible, especially at the core of the scanner. However, a little inhomogeneity is always left. Even with an ideal magnet, inhomogeneity will be caused by the susceptibility of the object being imaged. Magnetic permeability is given by $\mu = \mu_0(1+\chi)$ where χ is called susceptibility. Most of human tissues are diamagnetic, i. e., $\chi < 0$ for them. Their susceptibilities slightly change from issue to issue. These changes cause some small but sharp changes in magnetic field across the interface of two issues, especially in edges or tips. As static magnetic field in MR

scanners is strong, few parts per million (ppm) changes of field strength results in a considerable frequency shift in Larmor frequency and ultimately in image distortion.
According to Maxwell equations, for the static magnetic field with no electrical current, curl of magnetic field equals zero inside a uniform environment with constant χ. So scalar function V_m may be defined so that:

$$\vec{B} = -\mu \nabla V_m \tag{1}$$

where $\vec{B}$ is the magnetic field and V_m is called magnetic voltage. As $\vec{B}$ is divergence free, it yields to Laplace equation for V_m:

$$\nabla^2 V_m = 0 \tag{2}$$

which is valid for all points but the boundary points for which boundary condition must be used:

$$B_{n1} = B_{n2} \tag{3}$$

$$\frac{1}{\mu_1} B_{t\,1} = \frac{1}{\mu_2} B_{t2} \tag{4}$$

where subscriptions *n*, *t* show normal and tangential directions respectively.
Knowing boundary location, magnetic voltage can be calculated by equations (2) to (4) and then magnetic field may be derived from (1).

As water constitutes 70% of the human body, its susceptibility, which is -5.0×10^{-6} is a good approximation of body issues susceptibility. Li et al. [7] have used this permeability for all tissues except for air filled cavities like sinuses, lungs and stomach where they have used permeability of air and have shown the validity of this approximation. In this research, we have used the same method and therefore with a simple threshold setting we can automatically determine boundaries which are needed for equations (3) and (4) and form a so-called shape matrix.

2.2 Effects of field inhomogeneity in SE

Effects of inhomogeneity can be discussed under two categories. First is geometrical distortion, which means displacement of the pixel locations. Displacements up to 3 to 5 mm have been reported that are important for some cases as stereotactic surgery. Second problem is the undesired changes in the intensity or brightness of pixels, which may cause problems in determining different issues and reduce the maximum achievable resolution.
In this research, we focus on Spin Echo imaging, whose pulse sequence is shown in Figure 1. It shows *z* as the slice selection direction, *x* as the frequency encoding direction and *y* as the phase encoding direction.

As discussed in [4], static field inhomogeneity will cause changes in *z* and *x* directions so we have to use x_1 and z_1 instead, which contains the effects of inhomogeneity. As a simplified state, relations will be as follows:

$$x_1 \equiv x + \frac{\Delta B(x,y,z)}{G_x} \tag{5}$$

$$z_1 \equiv z + \frac{\Delta B(x,y,z)}{G_z} \tag{6}$$

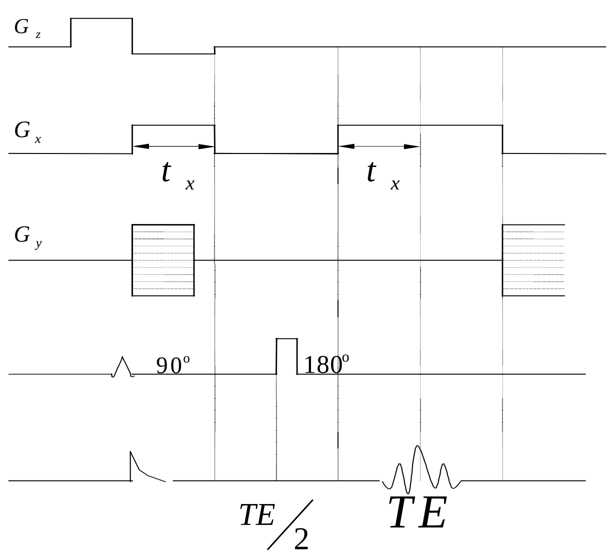

Fig. 1. Spin Echo pulse sequence.

where G_x and G_z are the gradient strengths in the *x* and *z* directions and ΔB is the deviation of static magnetic field from what it should be. Formulation of SE pulse sequence results in a change of intensity of pixels as follows:

$$i_1(x_1, y, z_1) = \frac{i(x, y, z)}{J(x, y, z)} \quad (7)$$

where i_1 is the new intensity, *i* is the real intensity and *J* is the Jacobean of this transformation which in this simple case is:

$$J(x, y, z) = 1 + \frac{1}{G_x} \cdot \frac{\partial \Delta B}{\partial x} + \frac{1}{G_z} \cdot \frac{\partial \Delta B}{\partial z} \quad (8)$$

equations (5), (6) and (8) show that as gradient strengths increase, both geometrical and intensity distortions decrease.

2.3 Finite Difference Method for inhomogeneity calculation

Finite Difference Method (FDM) is a well-known effective method for solving electromagnetic problems. Formulation and meshing in FDM is much easier than Finite Element Method (FEM), especially for digital images with rectangular pixels. We have used pixel corners as nodes of FDM mesh and as discussed before, boundaries can be determined automatically. For solving the Laplace equation, Gauss-Seidel method has been used. The only important point is how to implement boundary conditions, especially at edge points, which are treated in electromagnet theory as singularities. As we showed in [9] for a singular point seen in Figure 2, the following equation will generate a good approximation for the boundary condition:

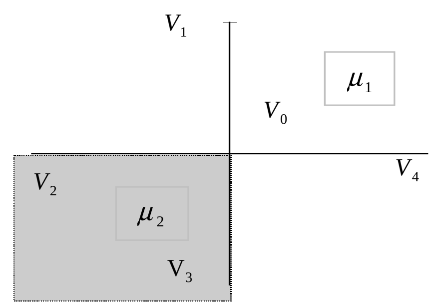

Fig. 2. a singular point with magnetic voltages. Gray area shows tissues where white area shows air filled environment.

$$V_0 \approx \frac{1}{2(3\mu_1 + \mu_2)} \left((\mu_1 + \mu_2) \cdot (V_2 + V_3) + 2\mu_1 (V_1 + \cdot V_4) \right) \quad (9)$$

where μ_1 and μ_2 are relative permeability of the two environments, respectively.

A multi-resolution method was applied to increase speed of convergence while preserving the accuracy by considering a large grid with boundaries far from the object. Speed of this method for a 128×128 picture with a simple processor by the clock pulse speed of 200 MHz takes only 90 seconds.

3. METHODS

3.1 Simulation of inhomogeneity artifact

We developed a method for which we need the value of the magnetic field variations at the corners of each pixel of the image, which can be calculated by the method described above. Once this inhomogeneity map has been obtained, we can shift each pixel corner to its new position in the frequency encoding direction as explained by equation (5).

As stated in Section 2, Jacobean of this transform causes the distortion in the intensity of the image. It means that because of the stretch or contraction of a pixel, its intensity spreads in a different area and so it will be attenuated or intensified, respectively. Therefore, shifting each pixel corner to its new position and then dividing previous intensity of each

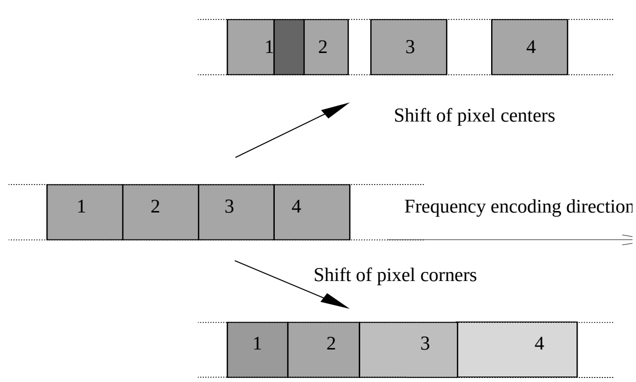

Fig. 3. Comparison of center shifting with corner shifting for inhomogeneity modeling.

pixel to its new area performs the role of Jacobean with no more calculation. This is one of the advantages of working with pixel corners rather than its center. The other advantage is that there will be neither overlap nor gap between pixels, as it is shown in Figure 3 for a simple case. This point is important not only in precision of simulation but also in being one to one and therefore reversibility of the transform.

This displacement in a more accurate way is shown in Figure 4, where each point has its own displacement in the frequency-encoded direction. For example, in the new image (bottom) pixel number 2 ($c'e'f'd'$) is built by partials of pixels 1 and 2 in the primary (undistorted) image, i.e., $c'cdd'$ and $ce'f'd$. Considering the area of $c'cdd'$ beside $acdb$ (in the new figure) as f_1 and the area of $ce'f'd$ beside $cefd$ as f_2, intensity of the pixel number 2 in the new image is calculated by:

$$i_2' = i_1 \times f_1 + i_2 \times f_2 \qquad (10)$$

where i_1 and i_2 are intensities in the first and second pixels of the primary image, respectively.

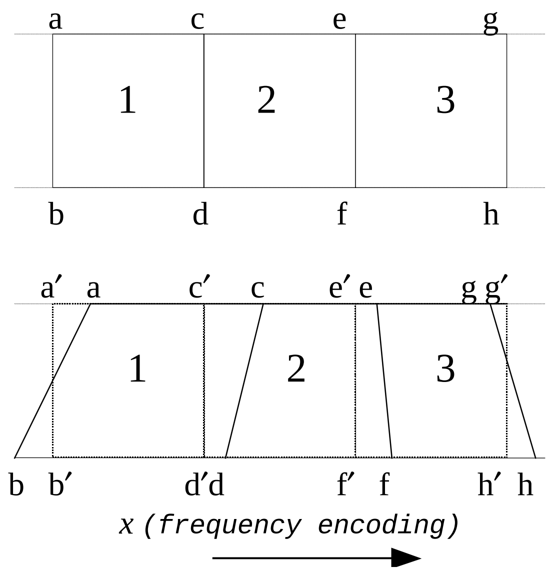

Fig. 4. Pixels deformations caused by corner shifting method. (top) undistorted image pixels, (bottom) distorted image.

3.2 Correction methods

In real imaging, the undistorted image is sought having the distorted image. In other word, first row of the figure 4 should be rendered from second row, with its distorted geometry and intensity. Having the magnetic inhomogeneity map, for each pixel, same process of simulation can be performed in reverse direction. It means that inhomogeneity term transferred to the other side of equation (5). It should be noted that inhomogeneity map is calculated from distorted image itself. This “direct” method, is very simple and easy, however, it has some problems especially near the edges of the image, where sharp magnetic changes happen. An example of the problem in this method is shown in Figure 5. Inhomogeneity effects on one row of primary image with just two gray scale levels, has been simulated with assumed displacement amounts (per pixel), which are shown in the picture. Boundary of two environments has been shifted to the left by one pixel and gray levels of pixels have also been changed. With the best assumption the field inhomogeneity map will not change and just will be shifted one pixel to the left. Next we have shown the direct correction method for removing these artifacts. Although the final result has improved in comparison with distorted position, both geometrical and intensity artifacts still exist, as it can be seen in the last row.

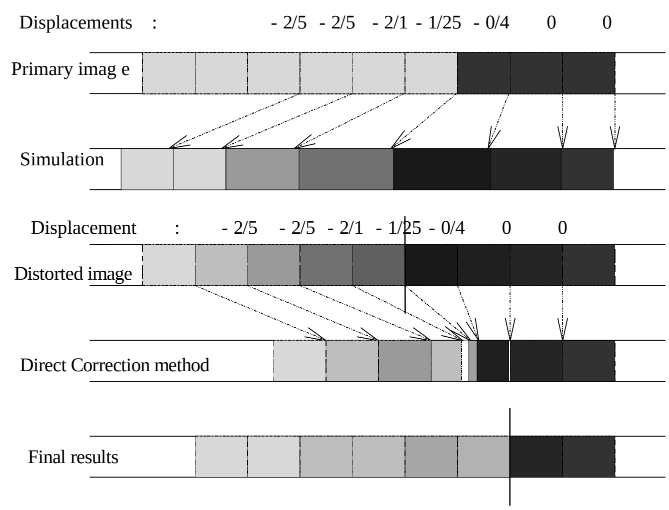

Fig. 5. Simulation of distortions caused by field inhomogeneity in SE and its schematic correction by direct (pixel based) method. Not complete Pixels deformations caused by corner shifting method.

To remedy this problem we can replace a grid base (indirect) method instead of this pixel based (direct) method. In the grid base method, we consider each node of the grid and having the field inhomogeneity in that point, we find the point that used to be in this point before distortion. That is, we find the amount and direction of the displacement and so locate the desired point in the distorted image and bring it back to its original place. Consequently, the intensity of the pixels will be modified using (10). Obviously, this method would be very accurate if we had the exact field map, however, the field map, which is derived from distorted image, will not be very accurate. As we examined, this method is very sensitive to the precision of the field map and with an inaccurate inhomogeneity map it may generate less accurate result compared to the direct method.

To remedy this problem of the indirect method, we first use the corrected geometry obtained by the direct method, which has shown good efficiency in removing geometrical distortions. Next the field inhomogeneity map is derived using this modified geometry and finally the indirect method is executed to generate the final image with modified intensity as well as geometry. The overall algorithm is shown in Figure 6.

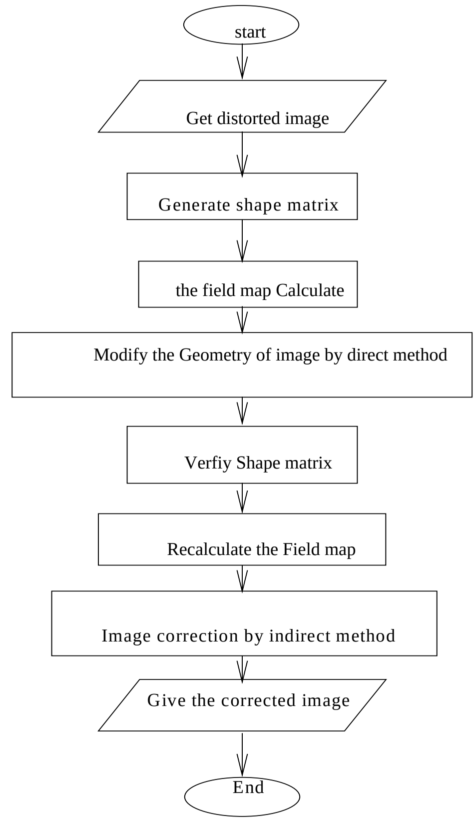

Fig. 6. Algorithm of indirect correction method.

4. RESULTS

4.1 Calculation and validation of field inhomogeneity

For a typical sagittal slice of the head, magnetic field distortion was calculated using the proposed method. The result was validated by comparing it to the map estimated by a Finite Elements method (FEM), which had been validated experimentally (Figure 7).

To have a quantitative validation, some small areas were chosen in both calculated maps and histograms of the field

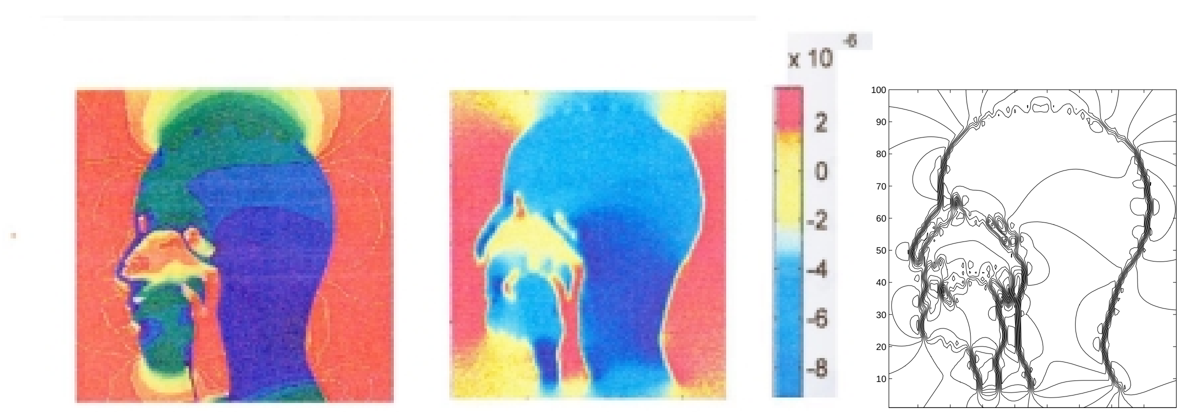

(a) (b) (c)

Fig. 7. Calculated magnetic field distortions through: (a) Finite Elements method and (b) proposed method. (c) calculated field contours.

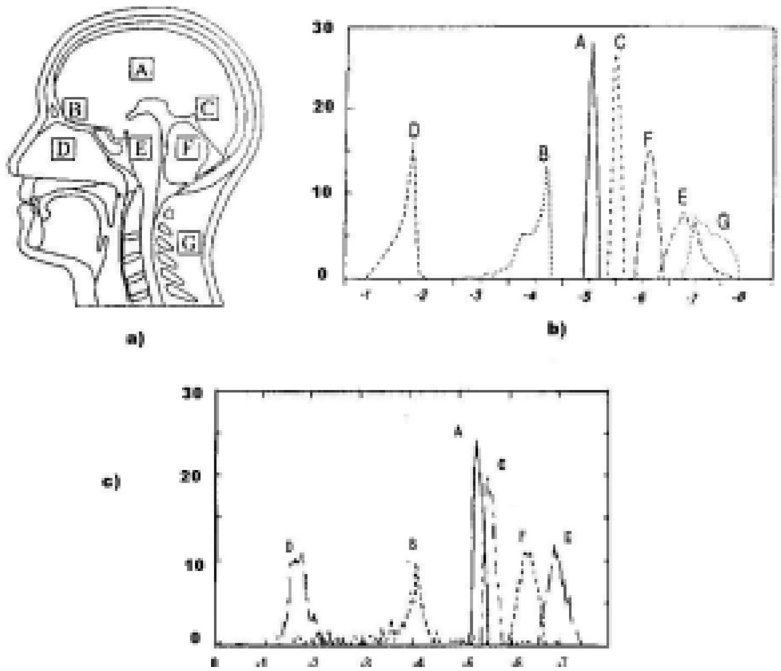

Fig. 8. a) Selected areas for comparison between two methods. b) Magnetic field inhomogeneity histogram, calculated from 2D Finite Element Method in selected areas. c) Corresponding histogram for the proposed method.

inhomogeneity as well as correlation coefficients between them presented in Figure 8 and Table 1. Just in area labeled E, correlation is moderate, however, the FEM also does not have a good agreement with the experimental measurement in this area [7] and cannot be an appropriate bench mark.

Table 1. Correlation coefficient between calculated field map from proposed method and FEM.

Area	A	C	E	F
Correlation Coefficient	0.97	0.85	0.52	0.97

4.2 Simulation of field inhomogeneity on SE images

We applied the procedure described by the proposed algorithm in Figure 5 on a simulated sagittal slice of the human head. Pixel size was assumed 2.5×2.5 cm and magnetic field gradient strength was set to 2.2 μ T/Pixel. All tissues are

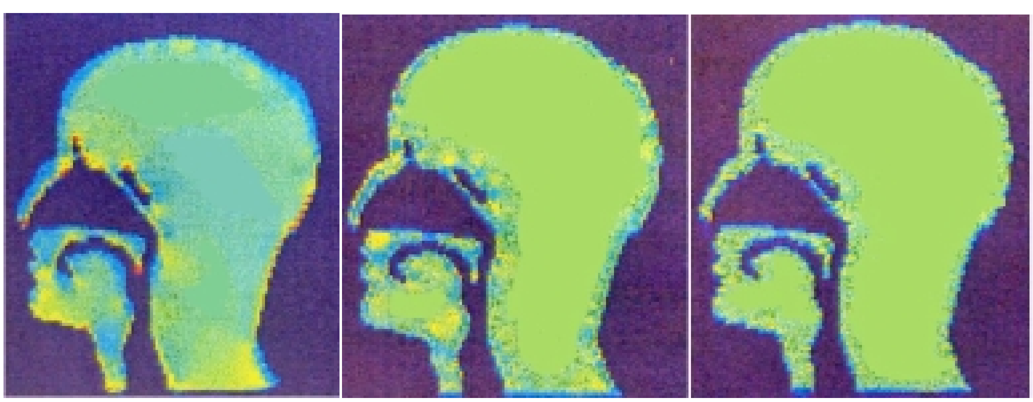

(a) (b) (c)

Fig. 9. (a) Simulated distorted image. (b,c) Corrected image from direct and indirect methods.

considered identical and therefore constant image intensity was expected. Then distortions were simulated by the proposed method. This distorted image (Figure 9 (a)) was used as an image we get from scanner. Using only this image, we tried to remove inhomogeneity artifacts by both direct and indirect methods. The results are compared in Figure 9.

4.3 Efficiency of correction methods

Both methods completely corrected geometrical distortions of the simulated image, however in real images some geometrical distortions may remain after the correction. Intensity correction was evaluated by comparing the corrected image with the undistorted image using equation (11):

$$RError = \frac{\sqrt{N \times \sum_{1}^{N} \Delta p_i^{\,2}}}{\sum_{1}^{N} p_i} \tag{11}$$

where Δp_i is the difference between the intensity of the ith pixel with its original value (p_i) and N is the number of the interior points of the model. The same procedure was repeated for the double resolution and for the double gradient strength and the resulting rms errors (equation (11)) are shown in Table 2.

Table 2. Efficiency of the correction methods under different conditions of resolution and magnetic field gradient strength.

	Error in distorted image	Error in corrected image by direct method	Percent of improvement in direct method	Error in corrected image by indirect method	Percent of improvement in indirect method
Normal state	0.139	0.474	66	0.314	78
Double Gradient strength	0.0454	0.0220	51.5	0.0204	55.1
Double resolution	0.1496	0.0646	56.8	0.0322	81.1

5. DISCUSSION

Table 2 shows that the indirect method outperforms the direct method for all cases examined. However, as this method is sensitive to the authenticity of the magnetic field map, if it is applied without prior geometrical correction, its performance degrades significantly. This table also shows that increasing the field gradient strength decreases the error in the acquired image and under this low artifact condition, the efficiency of the two methods are almost the same.

The other interesting result is obtained for the improved resolution. When pixel sizes were broken in half and other conditions remained unchanged, relative rms error of the distorted image did not show major changes. However, the direct method's efficiency fell while indirect method showed a slightly better performance. By looking at Figure 4 and comparing rows 2 and 3, we understand that the simulation process and also the indirect method (which is exactly the inverse of the simulation process) are more accurate in higher resolution. But row 4 shows that in direct method the intensities of different pixels may concentrate in one point and therefore in higher resolutions it may cause more sever problems.

6. CONCLUSION

In this study, based on node magnetic voltage values, a fast Finite Difference Method (FDM) is developed for susceptibility-induced mapping of the magnetic field inhomogeneity and applied to the simulated MRI data. Its accuracy and speed of convergence are evaluated by comparing the method to the Finite Elements method (FEM).

Effects of inhomogeneity on spin echo (SE) MRI are simulated using the proposed field calculation method. Also, a pixel based (direct) method as well as a grid based (indirect) method for removing the effects are developed. Magnetic field calculation, simulation and correction methods, all are performed using corners of the image pixels rather than their centers, simplifies the procedure.

The high speed of the algorithm stems from its multi-resolution nature. The main advantage of the proposed method is that it does not need any data except for the image itself and the inhomogeneity map can be generated automatically from the MR image.

Both correction methods remove geometrical distortion almost completely. The indirect method shows a better performance over the direct method in removing intensity errors, especially in higher resolutions and larger rms errors. However, the indirect method is more sensitive to the accuracy of the inhomogeneity map.

7. REFERENCES

1. Y.M. Kadah, X. Hu, "Simulated Phase Evolution Rewinding (SPHERE): a technique for reducing B_0 inhomogeneity effects in MR images," *Magn. Reson. Med.*, vol. 38, pp. 615-627, 1997.
2. J.R. Reichenbach, R. Venkatesan, D.A. Yablonskiy, M.R. Thompson, S. Lai, and E. M. Haacke, "Theory and application of static field inhomogeneity effects in Gradient-Echo imaging," JMRI, vol. 7, pp. 266-279, 1997.
3. C.J.G. Bakker, R. Bhagwandien, M.A. Moerland, L.M.P. Ramos, "Simulation of susceptibility artifacts in 2D and 3D fourier transform Spin-Echo and Gradient-Echo magnetic resonance imaging," *Magnetic Resonance Imaging*, vol. 12, No. 5, pp. 767-774, 1994.
4. H. Chang and J.M. Fitzpatrick, "A technique for accurate magnetic resonance imaging in the presence of field inhomogeneities," *IEEE trans. on Med. Imaging*, vol. 11, No. 3, September1992.
5. S. Li, G.D. Williams, T.A. Frisk, B.W. Arnold, M.B. Smith, "A computer simulation of the static magnetic field distribution in the human head," *Magn. Reson.Med.*, vol.34, pp. 268-275, 1995.
6. D.A. Yablonskiy and E.M. Haacke, "Theory of NMR signal behavior in magnetically inhomogeneous tissues: the static dephasing regime," *Magn. Reson.Med.*, vol.32, pp. 749-763, 1994.
7. Li, B.J. Dardziniski, C.M. Collins, Q.X. Yang, and M.B. Smith, "Three-Dimensional mapping of the static magnetic field inside the human head," *Magn. Reson.Med*., vol36, 705-714, 1996.
8. D.C. Alsop, and T.J. Connick, "Optimization of Torque-Balanced asymmetric head gradient coils," *Magn. Reson. Med.*35, pp. 875-886, 1996.
9. A.N. Moghaddam, "Analysis of Electromagnetic Fields Distribution in MRI systems in Human Head Presence," M.S. Thesis, Tehran University, MS thesis, October 1998.